Short communication

Transient extension and relaxation of a dilute polymer solution in a four-roll mill

J. Feng[a,*], L.G. Leal[b]

[a]*The Levich Institute, City College of New York, New York, NY 10031, USA*
[b]*Department of Chemical Engineering, University of California, Santa Barbara, CA 93106, USA*

Abstract

This note describes numerical simulations of transient extension-dominated flows of a dilute polymer solution in a four-roll-mill flow cell. When the roller speed changes abruptly, the polymer, modeled as an ensemble of FENE-CR dumbbells, experiences unusual transients in stretching and relaxation that are related to the inhomogeneity of the flow field. Since extensional flows generated in the laboratory are necessarily inhomogeneous, these numerical results may serve as guidelines for designing such experiments and interpreting the results. © 2000 Elsevier Science B.V. All rights reserved.

Keywords: Polymer solution; Extensional flows; FENE-CR model

1. Introduction

Extensional flows are a sensitive probe into the dynamics of polymer chains, and hence have been studied in several laboratories [1]. Of particular interest are transient extensional flows, which highlight the short-time-scale dynamics of the chains such as the appearance of a dissipative stress [2–4]. Homogeneous extensional flows are difficult to produce in the laboratory because the streamlines necessarily terminate on solid boundaries, and cannot diverge as is ideally the case. A popular apparatus is the filament stretching device which offers a reasonably large area of uniaxial elongation. Because of the exponential separation of the endplates, however, it is difficult to achieve large strains and steady-state stretching. Besides, the endplates introduce inhomogeneity and elastic decohesion [5,6]. The four-roll mill offers a possible alternative for studying transient extensional flows, with the obvious advantage that arbitrarily large strains can be easily attained. However, the flow is driven by the rollers, and control of the extensional rate is complicated by inhomogeneous kinematics, especially during rapid transients. The present simulations are motivated by such considerations. Though our
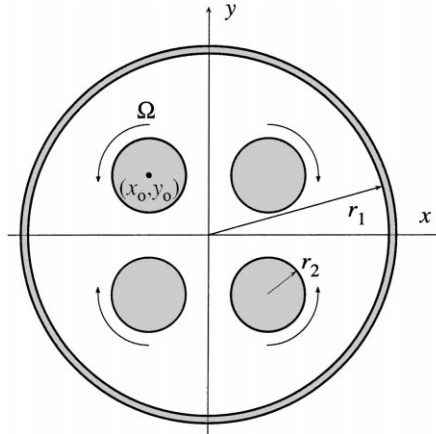
---

* Corresponding author.

0377-0257/00/$ – see front matter © 2000 Elsevier Science B.V. All rights reserved.
PII: S 0 3 7 7 - 0 2 5 7 (9 9) 0 0 0 5 2 - X

Fig. 1. Geometry of the four-roll mill device. $r_2/r_1 = 0.204$, $(x_0, y_0) = (-0.33, 0.33)r_1$.

interest lies more in entangled solutions and melts [7], we used the FENE-CR model as a first step because the constitutive laws appropriate for concentrated solutions are still being developed and complex flow calculations cannot be done with the same confidence.

Flow of dilute polymer solutions in the four-roll mill has been studied in a recent paper [8], but its emphasis was on steady-state flows. The geometry of the problem is shown in Fig. 1. When the rollers rotate in the indicated direction with the same angular velocity, a planar extensional flow is generated near the stagnation point at the center. We will investigate the reaction of the polymer when this angular velocity changes abruptly. Four flow situations will be studied: abrupt start and stop of the rollers and stepwise increase and decrease of the roller speed. Because of symmetry, only one-quarter of the domain needs to be computed; we have chosen the second quadrant.

The FENE-CR model and the numerical techniques that we use here have been described in [8]. For the Stokes flow of a Newtonian fluid, the angular velocity of the roller Ω is linearly related to the elongation rate at the stagnation point $\dot{\gamma}_N$. If we use r_1 as the characteristic length, $r_1\dot{\gamma}_N$ as the characteristic velocity and $\dot{\gamma}_N^{-1}$ as the characteristic time, the governing equations can be made dimensionless:

$$\nabla \cdot \boldsymbol{u} = 0,$$

$$\mathrm{Re}\frac{\partial \boldsymbol{u}}{\partial t} = -\nabla p + \nabla^2 \boldsymbol{u} + \frac{c}{\mathrm{De}}\nabla \cdot (f\boldsymbol{A}),$$

$$\frac{\partial \boldsymbol{A}}{\partial t} + \boldsymbol{u} \cdot \nabla \boldsymbol{A} - (\nabla \boldsymbol{u})^{\mathrm{T}} \cdot \boldsymbol{A} - \boldsymbol{A} \cdot \nabla \boldsymbol{u} = \frac{f}{\mathrm{De}}(\boldsymbol{I} - \boldsymbol{A}),$$

where $\boldsymbol{A}$ is the polymer configuration tensor, $\boldsymbol{I}$ is the unit tensor, and

$$f = \frac{1}{1 - \mathrm{Tr}\boldsymbol{A}/L^2},$$

for the nonlinear Warner spring. The trace of $\boldsymbol{A}$, $\mathrm{Tr}\,\boldsymbol{A}$, gives a measure of the average length of the chains. The Reynolds number is defined using the solvent viscosity: $\mathrm{Re} = \rho r_1^2 \dot{\gamma}_N/\mu_s$ and the Deborah

number using the relaxation time of the spring: $De = \lambda \dot{\gamma}_N$. The strain-rate $\dot{\gamma}$ is defined as $\dot{\gamma} = (\boldsymbol{D}:\boldsymbol{D}/2)^{1/2}$ where $\boldsymbol{D} = [\nabla \boldsymbol{u} + (\nabla \boldsymbol{u})^T]/2$ is the rate of strain tensor. The parameters used in the simulations are $L = 20$, $c = 0.1$; see [8] for a brief discussion on the choice of parameter values. Re and De vary with the roller speed Ω and will be specified below. The Reynolds number is typically small in the corresponding experimental system. Thus, the inertial terms in the equation of motion can be neglected for all but a short time following the change in roller speed during which the time derivative term Re $\partial \boldsymbol{u}/\partial t = O(1)$ and is not negligible. This time is on the order of O(Re), which is also the time scale for viscous diffusion in the flow cell. We thus retain the time derivative term but neglect the nonlinear convective term in the inertia. In practice, however, the time derivative hardly has any effect on the results for the small Re values that we have used. This is because the vorticity diffusion time is much smaller than the viscoelastic time scale on which the polymer configuration and the concomitant flow modification evolve.

2. Abrupt start and stop

The roller starts to rotate at time $t = 0$ with an angular velocity that corresponds to $De = 1.34$ and $Re = 0.136$. After a steady state is established, the roller abruptly stops at $t = 20$. Histories of the polymer stretching Tr $\boldsymbol{A}$ and the strain-rate $\dot{\gamma}$ at the stagnation point are shown in Fig. 2.

Shortly after the flow starts, the strain-rate jumps to the steady-state Newtonian value $\dot{\gamma}_N$. This process is via viscous diffusion and is fast owing to the low Reynolds number. Note that the sole role of
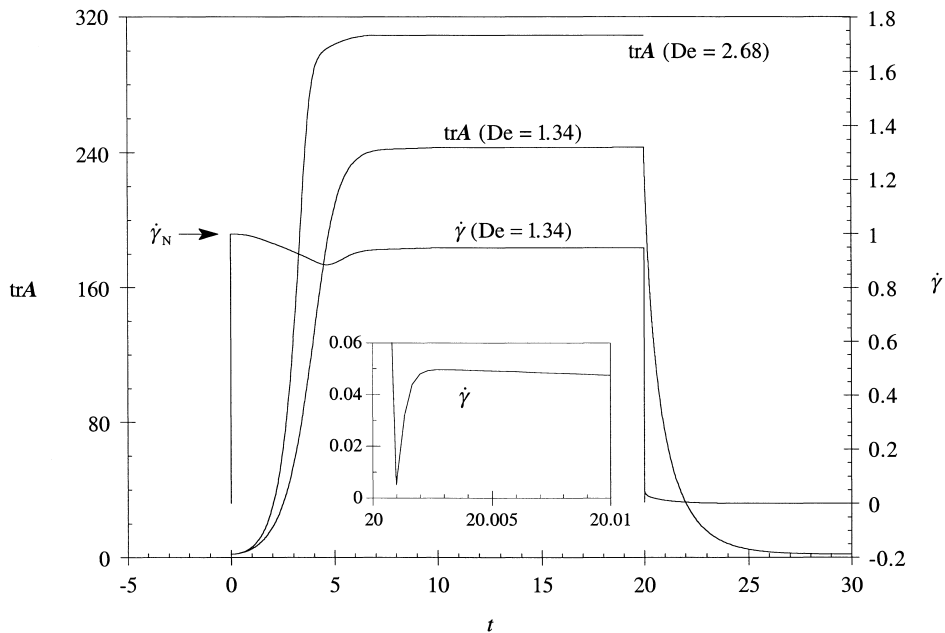

Fig. 2. Transients of Tr $\boldsymbol{A}$ and $\dot{\gamma}$ at the stagnation point with the rollers starting abruptly at $t = 0$ and then stopping at $t = 20$. $\dot{\gamma}$ is scaled by the Newtonian value $\dot{\gamma}_N$ corresponding to the same roller speed and t is scaled by $\dot{\gamma}_N^{-1}$. The inset shows details of the rebound in $\dot{\gamma}$ after the rollers stop. A startup curve for $De = 2.68$ is also shown which will be referred to in the next section.

Re is to set the time-scale for viscous diffusion, which does not interfere with the transients of interest as long as Re is small. As the polymer starts to stretch, the elongational viscosity increases (strain-hardening), causing $\dot{\gamma}$ to decrease before approaching its steady-state value of $0.948\dot{\gamma}_N$. In the meantime, the polymer stretches *monotonically* to a steady state. We will return to this point when discussing the step increase in roller speed. One may notice that the steady-state Tr A value is somewhat smaller than that corresponding to a uniform planar extension at the same De. This is because our De is defined using a nominal strain-rate $\dot{\gamma}_N$ that is higher than the true steady-state strain-rate at the stagnation point.

When the rollers are brought to a sudden halt, the strain-rate $\dot{\gamma}$ initially drops to zero, again through rapid viscous diffusion. Then as the polymer starts to relax, $\dot{\gamma}$ experiences a small but distinct rebound before finally dying out (see inset). This rebound is due to a 'residual flow' driven by the polymer stress field. Fig. 3 plots the velocity components u along the x-axis and v along y-axis at different times. After the rollers stop, the velocity drops to zero almost immediately. Then a *reverse flow* develops, which, according to the inset in Fig. 2, reaches its peak around $\tau = 0.003$. Among the velocity profiles captured in Fig. 3, the strongest reverse flow occurs at $\tau = 0.01$. The subsequent decay of the reverse flow is on a time scale consistent with the polymer's relaxation. This behavior is reminiscent of the 'constrained recoil' described by Bird et al. [9]. In fact, a similar elastic recoil has been experimentally documented by Pakdel et al. [10] in a lid-driven cavity flow of a Boger fluid after the lid stops suddenly. The recoil also dies out on the scale of the fluid's relaxation time.

In our simulations, the recoil is most prominent within the 'birefringence strand' along the y-axis, where the polymer stretching is the greatest before the rollers halt [8]. The streamlines in Fig. 4 offer a global picture of the reverse flow; the asymmetry between the x and y axes contrasts with the near
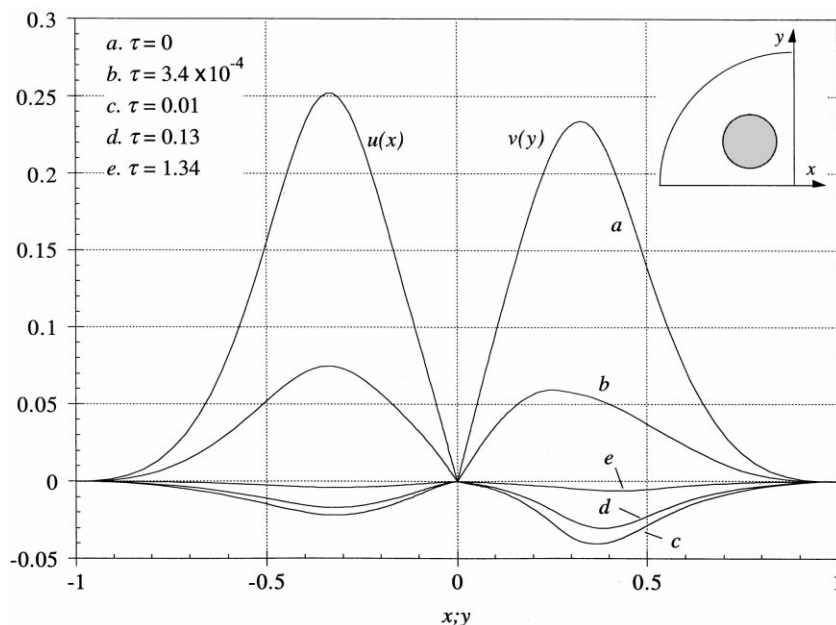

Fig. 3. Reverse flow: evolution of the velocity profiles $u(x)$ and $v(y)$ after the rollers stop. τ measures the time after the stop.
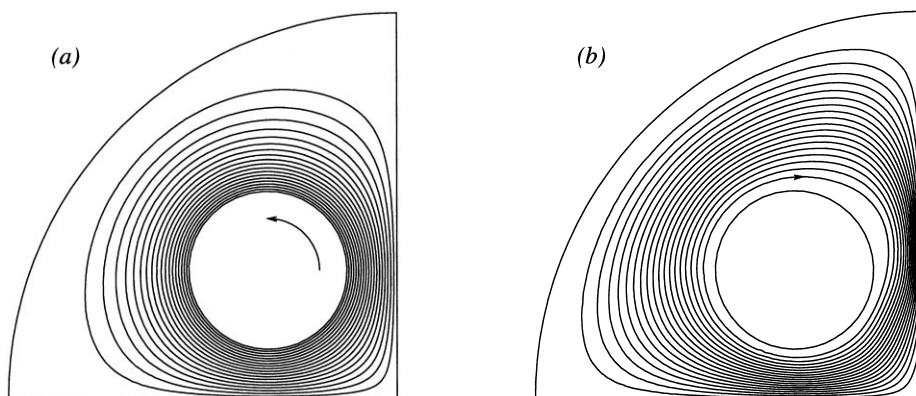
Fig. 4. (a) Streamlines of the steady-state flow at De = 1.34. The roller rotates counterclockwise. (b) Streamlines of the reverse flow at $\tau = 0.01$ after the roller halts.

symmetry of the steady state. The streamlines also confirm that the maximum retraction velocity occurs on the *y*-axis. At the stagnation point, the reverse flow has only a small effect on $\dot{\gamma}$ and hardly any effect on the relaxation of the polymer chains. We have computed the reaction of Tr A to an instantaneous cessation of a homogeneous extensional flow and it follows the relaxation in Fig. 2 almost exactly.

3. Stepwise changes in the roller speed

Fig. 5 shows the dynamics at the stagnation point when the roller speed abruptly doubles from De = 1.34 to 2.68, and after attaining steady state, steps back down to De = 1.34.

As compared with the startup in Fig. 2, the strain-rate has a similar transient after the roller speed doubles. However, Tr A experiences an overshoot and an undershoot here while the stretching is monotonic after the startup. The transient is not an inherent feature of the FENE-dumbbell polymer dynamics. Rather, it is a result of the coupling between the flow and the polymer stretching. For startup, the polymer is initially in the equilibrium coiled state and the spring is soft. The long relaxation time ensures that the polymer stretching does not respond quickly to the flow field. Moreover, transients in the flow may not be reflected by the polymer configuration since the latter depends on an integration over the flow history. When the strain-rate dips in Fig. 2, the polymer is far from its steady-state configuration, and hence keeps on stretching. This is why Tr A shows no overshoot after startup. In fact, if the rollers start directly from rest to De = 2.68, the polymer still stretches monotonically (see Fig. 2). In contrast, when the roller speed doubles from De = 1.34 to 2.68, the ground state is already a well-stretched one, and the nonlinear Warner spring has a short relaxation time and a fast response to the flow. Thus, when the strain-rate shoots up, so does the polymer stretching with little delay. Now when the strain rate decreases in response to the increased elongational viscosity, Tr A follows closely and hence the overshoot and the subsequent undershoot. The dashed line in Fig. 5 shows the response of the polymer to a perfect square-wave change in $\dot{\gamma}$; the stretching and relaxation are both monotonic. Therefore, the overshoot and undershoot in Fig. 5 are not due to the polymer dynamics per se, as is the case for more concentrated solutions [11]. Instead, it is a result of the flow-polymer coupling in this inhomogeneous extensional flow.
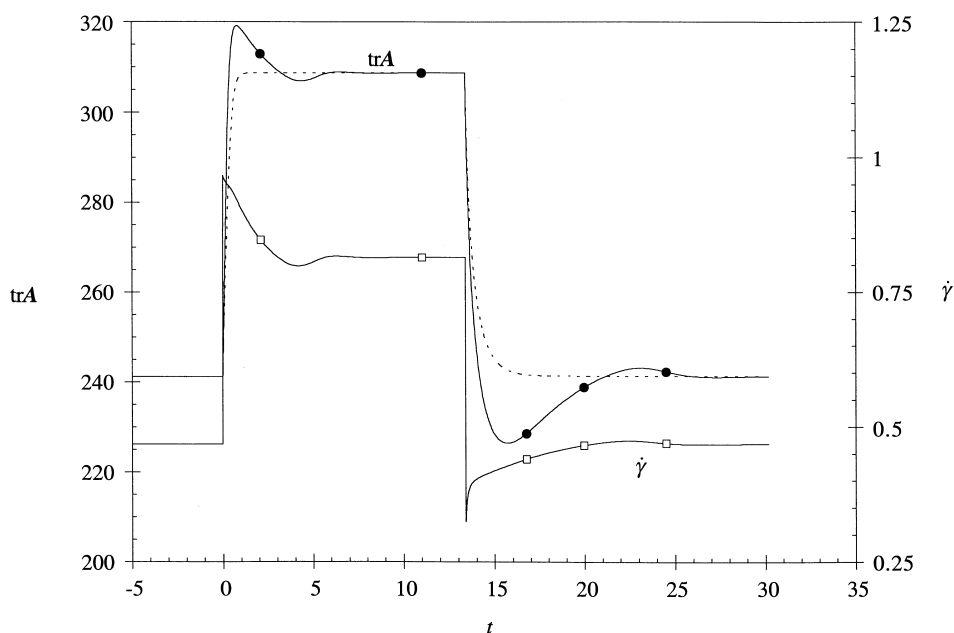
Fig. 5. Transients of Tr A and $\dot{\gamma}$ at the stagnation point with the roller speed doubling at $t = 0$ and then halving at $t = 13.4$. The dashed line represents the response of Tr A to a perfect square-wave change in $\dot{\gamma}$.

The transient following a sudden halving of the roller speed also differs from the monotonic relaxation in Fig. 2, and can be understood in the same fashion as for the abrupt doubling of the roller speed. Note that the transient after the step-down is somewhat slower than that after the step-up — another indication of the nonlinear spring effect.

4. Concluding remarks

The simulations reported here show rather unexpected transients in a four-roll mill following abrupt changes in the roller speed. These are caused by the interplay between the fluid flow and polymer configuration, and are ultimately a result of the inhomogeneity of the flow field.

If the four-roll mill is used as an extensional rheometer, one needs to be wary of spurious transients in the birefringence. The local strain-rate at the stagnation point should be measured in the same time in order to interpret the birefringence data. Note that the greatest effect of flow-polymer coupling occurs in the birefringence strand downstream of the stagnation point. Thus, if the measuring area is kept small at the stagnation point, data contamination is limited. The simulations are for a small concentration parameter $c = 0.1$, which corresponds to an exceedingly dilute solution. As the concentration increases, all the gradients in the flow field will be smoothed and the effects described here will be less conspicuous. Obviously, a more definite assessment of the four-roll mill as a transient extensional flow device requires more detailed experimental and numerical studies using solutions of various concentrations. We hope that the phenomena reported here will serve as an indication and guideline for such investigations.

Acknowledgements

References

[1] D.F. James, K. Walters, A critical appraisal of available methods for the measurements of extensional properties of mobile systems, in: A.A. Collyer (Ed.), Techniques in Rheological Measurements, Ch. 2, Chapman and Hall, London, 1993.

[2] J.M. Rallison, Dissipative stresses in dilute polymer solutions, J. Non-Newtonian Fluid Mech. 68(6) (1997) 1–83.

[3] N.V. Orr, T. Sridhar, Stress relaxation in uniaxial extension, J. Non-Newtonian Fluid Mech. 67 (1996) 77–103.

[4] S.H. Spiegelberg, G.H. McKinley, Elastic and viscous contributions to stress in extensional rheometry of viscous polymer solutions, in: Proc. 11th Int. Congr. on Rheology, 1996, Quebec City, pp. 211–212.

[5] S.H. Spiegelberg, D.C. Ables, G.H. McKinley, The role of end-effects on measurements of extensional viscosity in filament stretching rheometers, J. Non-Newtonian Fluid Mech. 64 (1996) 229–267.

[6] S.E. Spiegelberg, G.E. McKinley, Stress relaxation and elastic decohesion of viscoelastic polymer solutions in extensional flow, J. Non-Newtonian Fluid Mech. 67 (1996) 49–76.

[7] J.P. Oberhauser, D.W. Mead, L.G. Leal, The response of entangled polymer solutions to step changes of shear rate: signatures of segmental stretch?, J. Polym. Sci. Polym. Phys. Ed. 36 (1998) 265–280.

[8] J. Feng, L.G. Leal, Numerical simulations of the flow of dilute polymer solutions in a four-roll mill, J. Non-Newtonian Fluid Mech. 72 (1997) 187–218.

[9] R.B. Bird, R.C. Armstrong, O. Hassager, Dynamics of Polymeric Liquids, Vol. 1. Fluid Mechanics, Sec. 3.4, Wiley, New York, 1987.

[10] P. Pakdel, S.H. Spiegelberg, G.E. McKinley, Cavity flows of elastic liquids: two-dimensional flows, Phys. Fluids 9 (1997) 3123–3140.

[11] E. Geffroy, L.G. Leal, Flow birefringence studies of a concentrated polystyrene solution in a two-roll mill. I. Steady flow and start-up of steady flow, J. Polym. Sci. Part B: Polym. Phys. 30 (1992) 1329–1349.